Volume 5, Issue 12, December 2015 ISSN: 2277 128X
International Journal of Advanced Research in Computer Science and Software Engineering
Research Paper
Available online at: www.ijarcsse.com

Numerical Study of the Polarization Direction Effect on the Optical Properties of Gold Nanorods in Dielectric Medium

Z. Bassam, A. Akouibaa, A. Derouiche, S. El-fassi
Polymer Physics and Critical Phenomena Laboratory, Research Center: Materials and Energy, Sciences Faculty Ben M.Sik, P.O. BOX 7955, Casablanca, Morocco

Abstract—Gold nanorods (GNRs) have recently attracted widespread attention due to their unique optical properties and facile synthesis. In particular, they can support a longitudinal surface plasmon, which results in suspensions of them having a strong absorption peak in the upper visible or near-infrared parts of the spectrum. Due to recent advances in controlling the surface chemistry of these particles through functionalization there is a great deal of interest in using gold nanoparticles as selective biomarkers in biodiagnostics or for selective targeting in photothermal thearapeutics. In this work the polarization direction dependent optical response and dielectric permittivity of the GNRs is calculated using the Finite Element Method (FEM). The numerical obtained results show that the peak position of the surface plasmon resonance (SPR) and dielectric permittivity depends on the orientation of the GNR relative to the polarization field direction.

Keyword—Gold nanorods, Drude critical points model, Surface Plasmon Resonance, finite element method

I. INTRODUCTION

The optical properties of metal nanoparticles are dominated by surface plasmon resonances (SPR) (i.e., collective oscillations of conduction electrons in phase with an external electromagnetic wave).(e.g. [1]) The resonance frequency can be modulated through the composition, size, shape, and electromagnetic environment of the metal particles.(e.g. [2],[3]) Because of the large interest from both the scientific and technological points of view, the research on such metallic nanostructures has been tremendously intense during the past couple of decades. Gold nanoparticles can also convert optical energy into heat via non-radiative electron relaxation dynamics (e.g. [4]-[6]), endowing them with intense photothermal properties (e.g. [7]-[17]). Such localized heating effects can be directed toward the eradication of diseased tissue, providing a noninvasive alternative to surgery (e.g. [18]). Colloidal gold is well known to be biologically inert and has been used in vivo since the 1950s, namely as adjuvant in radiotherapies (e.g. [19]), but the consideration of such nanoparticles as photothermal agents is relatively recent.

Gold nanorods (NRs) are especially attractive for their highly efficient absorption in the near-infrared (NIR) region, a spectral window which permits photons to penetrate biological tissues with relatively high transmittivity. NRs with well-defined shapes and sizes are readily synthesized by seeded growth methods (e.g. [20],[21]), and their longitudinal plasmon resonances (LPRs) can be finely tuned as a function of aspect ratio. NRs support a larger absorption cross-section at NIR frequencies per unit volume than most other nanostructures and have narrower line widths due to reduced radiative damping effects, with consequently higher optothermal conversion efficiencies (e.g. [5]). The LPRs can also support nonlinear optical effects, such as a plasmon-enhanced two-photon luminescence (TPL) (e.g. [22]). Moreover, the LPRs are sensitive to the polarization of the incident excitation; by slightly adjusting the wavelength of a continuous-wave (cw) polarized laser, individual NRs could be aligned for several minutes in an optical trap (e.g. [23]). These properties give rise to many exciting possibilities to deploy NRs for biological imaging and photothermal therapy.

To describe the phenomenon of surface plasmon resonance of metal nanostructures several theories and methods have been developed in the recent years. Mie (e.g. [24]) first described this phenomenon theoretically by solving Maxwell's equations for a radiation field interacting with a spherical metal particle under the appropriate boundary conditions. The only material-related functions and constants in Mie's theory are the complex dielectric function of the metal and the dielectric constant of the surrounding medium. The plasmon absorption band also depends on the size of the particles and many attempts have been made to experimentally correlate the absorption maximum and the plasmon bandwidth to the actual particle size with overall moderate success. (e.g. [1],[25]-[26]). Gans (e.g. [27]) extended Mie's theory to prolate and oblate spheroidal particles averaged over all orientations. For gold nanorods the plasmon resonance then splits into two modes: one longitudinal mode along the long axis of the rod and a transverse mode perpendicular to the first. Maxwell-Garnett theory, (e.g. [1],[28],[29]) an effective medium theory, is also often used to describe the optical properties of metallic nanoparticles. Maxwell-Garnett theory computes the effective (complex) dielectric function of the composite material consisting of the metallic nanoparticles and the surrounding medium (host material). From this dielectric function the refractive index and the absorption can be calculated. The shape of the particles can be included in this theory by a screening parameter. Martin and *co-workers*,(e.g. [30]-[33]) have used and modified the Maxwell-Garnett theory to model the absorption spectra of gold nanoparticles with shapes that vary from oblate or pancakelike to prolate or needlelike. The gold nanorods are embedded in a porous aluminum oxide membrane, in which they are well

separated and aligned parallel to each other. The optical absorption spectrum shows only one plasmon band, which blue-shifts with increasing aspect ratio in agreement with the theoretical simulations.

Numerical techniques are designed to solve the relevant filed equation in the computational domain, subject to the boundary constraints imposed by the geometry. Without making a priori assumption about which field interaction are most significant, numerical techniques analyze the entire geometry provided as input. The finite element method (FEM) (e.g. [34]), which is a powerful numerical modeling tool, has been widely used for modeling electromagnetic wave interaction with complex materials. Recently, Benhamou *et al*. (e.g. [35]-[37]) have used this method to study the plasmonic resonance of gold nanoparticles with various sheep and morphology. In this paper, we use the FEM approach for computing the potential distribution in the composite material consisting of the GNRs without shell randomly oriented in a dielectric medium and to derive its effective dielectric constant, this parameter allowed us to calculate the absorption cross-section. We will study the effect of the polarization direction of the incident light on the optical and dielectric properties of GNRs dispersed in a dielectric medium.

II. DIELECTRIC FUNCTION OF GOLD

Dielectric function of any material consists of a real term ε' and an imaginary term ε'', the first determines the polarizability of a material in the presence of an electric field, and the second determines its intrinsic loss mechanisms (e.g. [38.]). For noble metals such as gold, complex dielectric function can be decomposed into two components (e.g. [39]-[41]). One component is the Drude free-electron term, and the second component is the substantial contribution of the bound or inter-band electrons.

Compared to silver, the optical properties of gold nanoparticles are more difficult to represent in the visible/near-UV region with an analytic model. The reason for that is the more important role in the latter played by inter-band transitions in the violet/ near-UV region. The gold nanostructures has at least two inter-band transitions at $\lambda = 470\text{nm}$ and $\lambda = 330\text{nm}$ that do play an important role and must be included explicitly if a realistic analytic model for $\varepsilon(\omega)$ is sought. A different type of analytic model for the two inter-band transitions in gold in the violet/near-UV region has to be included to achieve a reasonable representation of $\varepsilon(\omega)$ with a minimum set of parameters. It is possible to include a family of analytical models, called critical points for transitions in solids, which satisfy a set of minimum requirements (like Kramers-Kronig consistency) and reproduce most of the line shapes in $\varepsilon(\omega)$ observed experimentally.

Recently, a Drude two-critical points model (D-2CPM) has been used for the description the permittivity of gold in the $200-1000\,\text{nm}$ range (e.g. [42]).Following this model, the frequency-dependent optical properties of gold in the visible/near-UV range can be very well represented by an analytic formula with three main contributions, to wit,

$$\varepsilon_{D-2CP}(\omega) = \varepsilon_\infty - \frac{\omega_D^2}{\omega^2 + i\omega\gamma_D} + G_1(\omega) + G_2(\omega) \quad (1)$$

Where the first and second terms are the standard contribution of a classical Drude model with a high-frequency limit dielectric constant ε_∞, a plasma frequency ω_D, and a damping term γ_D, while $G_1(\omega)$ and $G_2(\omega)$ are the contributions from the aforementioned inter-band transitions (gaps). The latter have the following expressions:

$$G_{p=1,2}(\omega) = A_p\Omega_p\left(\frac{e^{i\Phi_p}}{\Omega_p - \omega - i\omega\Gamma_p} + \frac{e^{-i\Phi_p}}{\Omega_p + \omega + i\omega\Gamma_p}\right) \quad (2)$$

Where the symbols have the following meaning, A_p amplitude, Ω_p energy of the gap, Φ_p phase and Γ_p broadening.

In a comparative study with a model including 4 Lorentzian-pole pairs (L4) proposed by Hao *et al* (e.g. [43]), Vial *et al* (e.g. [44]) have shown that the Drude two-critical points model was able to accurately describe the dielectric functions of gold and silver, with fewer parameters to determine than the L4 model, and also a lower memory footprint when used in the FDTD method framework In the particular case of silver, the accuracy of D-2CPM is clearly better than that of L4, and this may be of great importance if one wishes to study plasmon propagation length, for example.

III. CALCULATION METHOD

The finite element method (FEM) is one of the most common methods today for solving partial differential equations, including Maxwell's equations that govern electromagnetic phenomena. It was initially used to solve the equations of elasticity and structural mechanics and later adapted to electromagnetism.

In this work we have interested in the determination of the plasmonic properties of nanocomposites in which the gold nanoparticles are dispersed in a dielectric medium. we used a method based on two major steps: The first consists of calculating the effective complex dielectric permittivity using the finite elements method, this permittivity is the sum of two contributions, the real part ε'_{eff}, which is related to the stored energy within the medium and the imaginary part ε''_{eff}, which is related to the dissipation (or loss) of energy within the medium:

$$\varepsilon_{eff} = \varepsilon'_{eff} + \varepsilon''_{eff} \quad (3)$$

The second step consists in calculating the absorption cross section using the components ε'_{eff} and ε''_{eff} of the effective permittivity, the maximum of the absorption corresponds to the surface plasmon resonance of the gold nanoparticles study.

3.1 Method

The detailed description of the FEM for determining the effective permittivity in the quasi-static limit can be found elsewhere (e.g. [45]). As both computing power and the efficiency of the FE computational method, it is becoming possible to investigate new composite materials through computer simulations before they have even been synthesized.

FE tool is used to compute the solution of Laplace equation by determining the electric field and potential distribution from the physical properties of different phases of the composite material. Recent works have shown that the FE method could be successfully applied to compute the effective permittivity of periodic composite materials (e.g. [46]). The basic scheme of the FE method is now briefly recalled.

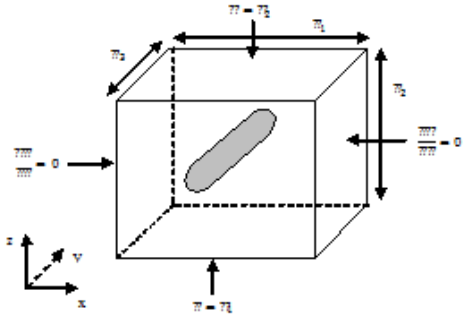

Fig. 1 Notation and boundary conditions related to a three-dimensional periodic nanocomposite. This cell contains a randomly oriented gold nanorod

To describe the FEM scheme, we consider a spatial domain, Ω, shown in Fig.1 with a vanishing charge density. Solving the problem at hand means finding the local potential distribution inside the computational domain by solving Laplace's equation (first principal of electrostatic):

$$\vec{\nabla}\left(\varepsilon_0 \varepsilon(\vec{r})\vec{\nabla}V(\vec{r})\right) = 0\,, \tag{4}$$

Where $\varepsilon(r)$ and $V(\vec{r})$ are the local relative permittivity and the potential distribution inside the material domain respectively with zero charge density. $\varepsilon_0 = 8.85.10^{-12}\ F/m$ is the permittivity of the vacuum. In addition, the composite (dielectric) is assumed to be periodic with three phases (metallic core, polymeric shell and host matrix). Taking into account the symmetry and periodicity properties, the geometry of the medium is reduced to a unit cell. The implementation of the FE method consists in dividing the three-dimensional domain into tetrahedral finite elements and interpolating the potential V and its normal derivative $\frac{\partial V}{\partial n}$ on each finite element similarly to the BIE method (e.g. [47],[48]) with the corresponding nodal values:

$$V = \sum_i \lambda_i V_i \tag{5}$$

$$\frac{\partial V}{\partial n} = \sum_i \lambda_i \left(\frac{\partial V_i}{\partial n}\right) \tag{6}$$

Where λ_i denotes the interpolating functions.

Following this analysis, the solution of Laplace's equation is obtained using the Galerkin method and by solving the resulting matrix equation from the boundary conditions thanks to a standard numerical technique, i.e., Gauss procedure (e.g. [34]).

Having computed the potential and its normal derivative on each tetrahedron of the computational mesh, the electrostatic energy W_e^k, and losses, P_e^k could be expressed for each tetrahedral element as:

$$W_e^k = \frac{\varepsilon_0}{2}\iiint_{V_k} \varepsilon_k'(x,y,z)\left[\left(\frac{\partial V}{\partial x}\right)^2 + \left(\frac{\partial V}{\partial y}\right)^2 + \left(\frac{\partial V}{\partial z}\right)^2\right] dV_k \tag{7}$$

$$P_e^k = \frac{\varepsilon_0}{2}\iiint_{V_k} \omega\varepsilon_k''(x,y,z)\left[\left(\frac{\partial V}{\partial x}\right)^2 + \left(\frac{\partial V}{\partial y}\right)^2 + \left(\frac{\partial V}{\partial z}\right)^2\right] dV_k \tag{8}$$

Where ε_k and V_k represent the permittivity and the volume of the k^{th} tetrahedron element, respectively. Thus, the total energy and losses in the entire composite can be written by summation over the n_k elements such as:

$$W_e = \sum_{k=1}^{n_k} W_e^k \tag{9}$$

$$P_e = \sum_{k=1}^{n_k} P_e^k \tag{10}$$

To compute quantities W_e and P_e, we suppose that the composite material is embedded in a plane capacitor. This way allows us to determine the effective permittivity in a direction parallel to the applied electric field. Then, from the capacitor electrostatic energy expression, we deduce the effective (complex) permittivity. We find that the real part, ε_{eff}', and imaginary one, ε_{eff}'', parallel to the applied electric field, are given by:

$$W_e = \frac{1}{2}\varepsilon_{eff}'\frac{S_d}{L_3}(V_2 - V_1)^2 \tag{11}$$

$$P_e = \frac{1}{2}\omega\varepsilon_{eff}''\frac{S_d}{L_3}(V_2 - V_1)^2\,. \tag{12}$$

Where V_1 and V_2 are the potentials applied across to plates of the unit cell (Fig. 1). Here, $S_d = L_1.L_3$ is the surface of in-depth. The real and imaginary parts of the effective permittivity then depends on the total energy, W_e, losses, P_e, linear size L_2 and applied potential difference $V_2 - V_1$. In addition, the second one is frequency-dependent. If the amplitude of the applied field is equal to 1, so the potential difference is kept equal to $\Delta V = L_2$. The following paragraph will be devoted to the determination of the optical properties of the material under investigation.

3.2 absorption cross-section

From the evolution of the effective complex dielectric function depending on the wavelength (or frequency) of the incident field, the resonance modes that may occur in nanoparticles are identified. For this, it would be interesting to

calculate the scattering cross-sections and absorption. The sum of these two quantities defines the extinction cross-section

$$\sigma_{ext} = \sigma_{abs} + \sigma_{diff}. \quad (13)$$

In the case where the dimensions are very small compared to the wavelength, the light scattering can be ignored, and we have: $\sigma_{ext} \approx \sigma_{abs}$

The cross-section of extinction *(absorption)* can be determined from the imaginary part of the effective dielectric function of the composite using the following equation (e.g. [49])

$$\sigma_{abs} = \frac{V_p}{f}\frac{k}{n_{eff}}\varepsilon''_{eff} \quad (14)$$

Here, V_p stands for the common volume of nanoparticles, f is their fraction, k is the wave-vector amplitude of the electromagnetic wave, and n_{eff} represents the refractive index that can be related to the real and imaginary parts, ε'_{eff} and ε''_{eff}, of the effective permittivity by (e.g. [50])

$$n_{eff} = \left(\frac{\sqrt{\varepsilon'^2_{eff}+\varepsilon''^2_{eff}}+\varepsilon'_{eff}}{2}\right)^{1/2} \quad (15)$$

This formula clearly shows that the peak of $\mathrm{Im}(\varepsilon_{eff})$ indicates that the light is rather absorbed in specific regions. The effective dielectric function and the effective refraction index are calculated using FEM. Hence, the section of optical absorption is easily obtained. In the following section, we present and discuss our findings.

IV. RESULTS AND DISCUTION

The aim of our work is to study the effect of the polarization direction on the dielectric and plasmonic properties of GNRs emerged in a non-absorbing dielectric medium. The polarization direction is determined relative to the principal axis of the NR. For this we consider an isolated GNR of height $h = 32nm$ and diameter $D = 8nm$. The aspect ratio of this nanoparticle is $\eta = 4$, defined by the ratio of height to diameter, with a volume fraction $\phi_v = 0.05$, the chosen permittivity of the host matrix is $\varepsilon_m = 1.77$. We assume that the field is applied following one direction making an angle θ with the direction of the long axis of GNR.

In Figs. 2 and 3, we report the evolution of real and imaginary parts of the effective permittivity upon the photon energy, for these curves we have varied the angle between the applied field direction and the GNR orientation from $\theta = 0°$ to $\theta = 90°$, and because of the distinction readability we have separately represented the curves corresponds to the angles $\theta = 0°$ to $\theta = 60°$ in Figs.2a and 3a, and for the angles $\theta = 60°$ to $\theta = 90°$ in Figs. 2b and 3b. These curves nicely illustrate the optical effects exhibited by small particles in the interface area mode. The imaginary part of the effective permittivity (Figs. 3a and 3b) allows to estimating the peak position of the resonance or extinction. The curves representing the real part ε'_{eff} (Figs 3a and 3a) show that in the vicinity of the SPR the value of ε'_{eff} rapidly falling from a maximum value ε'_{max} to a minimum value ε'_{max} , and the difference $\Delta\varepsilon'_{eff} = \varepsilon'_{max} - \varepsilon'_{min}$ decreases when the value of θ increases until it vanish for $\theta = 90°$. These curves also show that ε'_{eff} takes negatives values in a range of wavelengths when $\theta = 0°$ that is to say, when the direction of the polarization field is collinear with the major axis of NR, whereas this range reduces when the value of θ increases to a certain threshold where it disappear here at $\theta \approx 62°$. The negative values of ε'_{eff} opens the possibility of using these gold nanostructures in the design of metamaterials. These materials are often referred to as left handed materials or materials with negative refraction. Properties of such materials were analysed theoretically by Veselago long time ago (e.g. [51]), but only recently they were demonstrated experimentally (e.g. [52]). As was shown by Veselago (e.g. [51]), the left-handed materials possess a number of peculiar properties, including negative refraction for the interface scattering, inverse light pressure and reverse *Doppler* and *Vavilov-Cherenkov* effects.

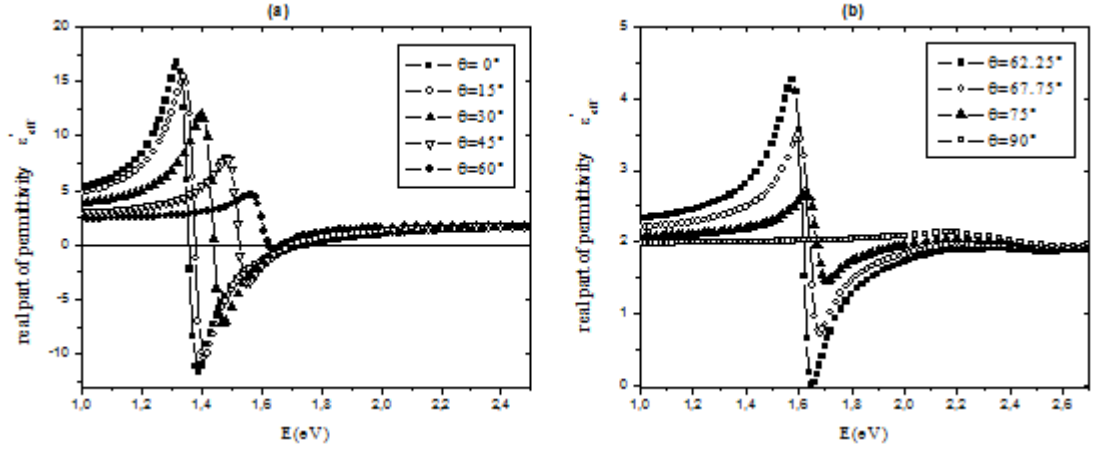

Figs.2a-2b. Evolution of the real part of the effective dielectric permittivity upon photon energy for different values of angle θ . The gold permittivity is described by the DCP model. For these curves, we choose: $\varepsilon_m = 1.77$, $\phi_v = 0.05$ and $\eta = 4$

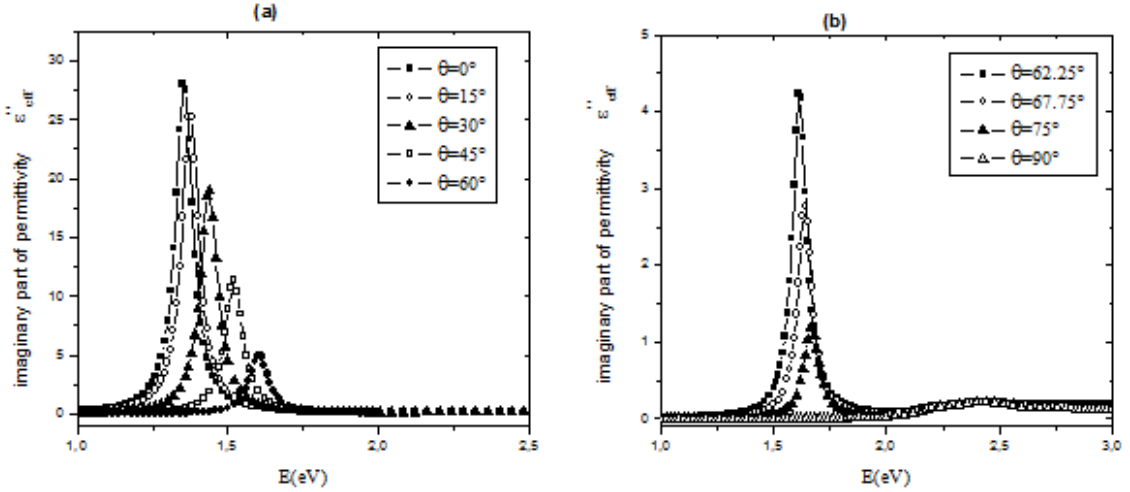

Figs.3a-3b. Evolution of the imaginary part of the effective dielectric permittivity upon photon energy for different values of angle θ . The gold permittivity is described by the DCP model. For these curves, we choose: $\varepsilon_m = 1.77$, $\phi_v = 0.05$ and $\eta = 4$

In Figs. 4a and 4b, we report the variation of the absorption cross-sections upon energy of the incident electromagnetic wave obtained using FEM. These curves show that when the direction of the external applied field is parallel to the major axis of the NR ($\theta = 0°$), the peak SPR place near the infrared (IR) wavelengths (here at $E = 1.37\text{eV}, \lambda_{max} = 906.22\text{nm}$) with an maximum absorption , in this case the excitation occurs along the axis of NR, this mode of excitation called longitudinal mode (L-mode). When the value of θ increases, the GNRs becomes inclined with respect to the polarization direction, in this case the position of the SPR peak of the longitudinal mode is shifted to the visible wavelength, ($E = 1.67\text{eV}, \lambda_{max} = 743.43\text{nm}$ for $\theta = 75°$) with remarkable decrease in absorption intensity. We note that, for a threshold value of θ (here at $\theta \approx 62°$) it begins to appear a second resonance peak in the vicinity of the blue wavelengths (here $E = 2.44\text{eV}, \lambda_{max} = 508.8\text{nm}$), this resonance peak corresponds to the transverse excitation of GNR that we calling transverse mode (T-mode). When ($\theta = 90°$) the polarization direction becomes strictly perpendicular to the GNR, in this case there is a total demise of the L-mode and the absorption spectrum contains only the transverse mode. To explain this different resonance mode we show in Fig.5 a Schema representing the transverse and longitudinal mode of oscillations of plasmons depending on the direction of electric vector of incident light. This scheme shows that when the external polarization field has a random direction relative to the GNR orientation, this field can be decomposed into two component, the first following the GNR major axis noted $\vec{E}_x$ and the second following the short axis noted $\vec{E}_y$, ie. $\vec{E} = \vec{E}_x + \vec{E}_y$. The component $\vec{E}_x$ is responsible to the excitation of longitudinal plasmons while the component $\vec{E}_y$ is responsible to the transverse plasmon excitation. We note that for the two extreme cases $\theta = 0°$ and $\theta = \frac{\pi}{2}$, one of the two components is zero thus we see the excitation of only one resonance mode.

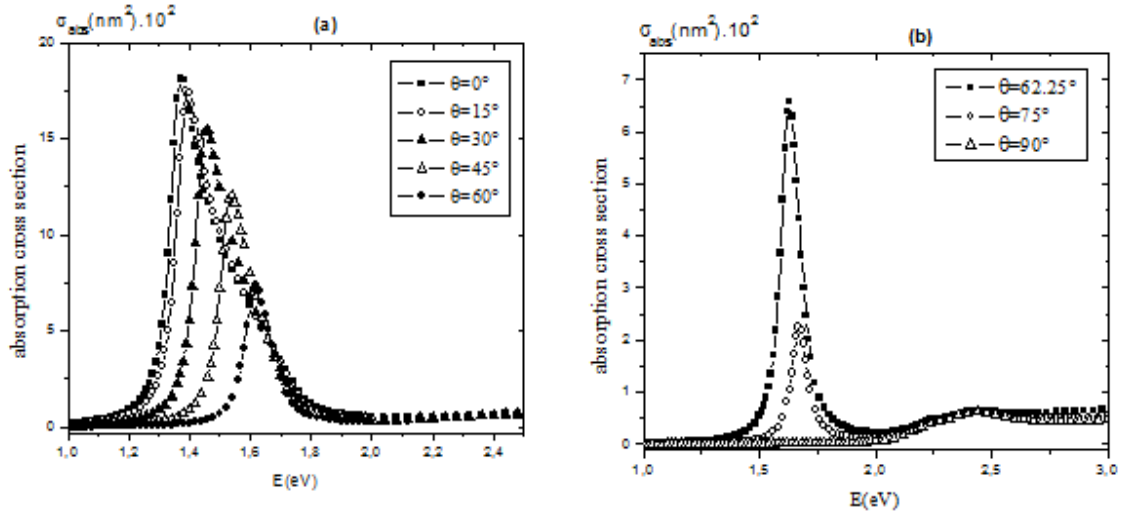

Figs. 4a-4b. Absorption cross-section, versus photon energy of gold nanorods for different values of angle θ. The chosen parameters are: $\eta = 4$, $\varepsilon_m = 1.77$ and $\phi_v = 0.05$.

It is important to note that the results obtained by our simulation method are in agreement with the experimental results obtained by Q. Liu *et al* (e.g. [53]), these authors realized the alignment of GNRs by nanoparticle self-assembly in liquid crystals (LCs) (e.g. [54]) through the LC-mediated realignment and rearrangement of incorporated nanoparticles in response to applied fields. These authors showed that the aligned GNRs in the LC matrix exhibit extinction spectra

varying with the angle between the polarizer and GNRs aligned along the major axis. These spectra have been obtained using a microscope with white light passing through a 4 mm^2 circular aperture, the glass cell with 1 mm gap between glass plates filled with the composite system of GNRs (10^{-8} M) in the shearing-aligned columnar hexagonal LC and then through a rotatable linear polarizer. The longitudinal SPR band is the strongest when the polarizer is parallel to the long axes of GNRs but decreases when the polarizer is perpendicular to GNRs long axes. In contrast, the transverse SPR peak is the strongest when the polarizer is orthogonal to GNRs long axes but becomes partially suppressed when rotating the polarizer toward the major axis of GNRs. The polarization sensitivity of the transverse SPR band is less pronounced than that of the longitudinal one. The SPR peaks of GNRs in LCs are slightly shifted to longer wavelengths as compared to the isotropic dispersions of the same nanorods.

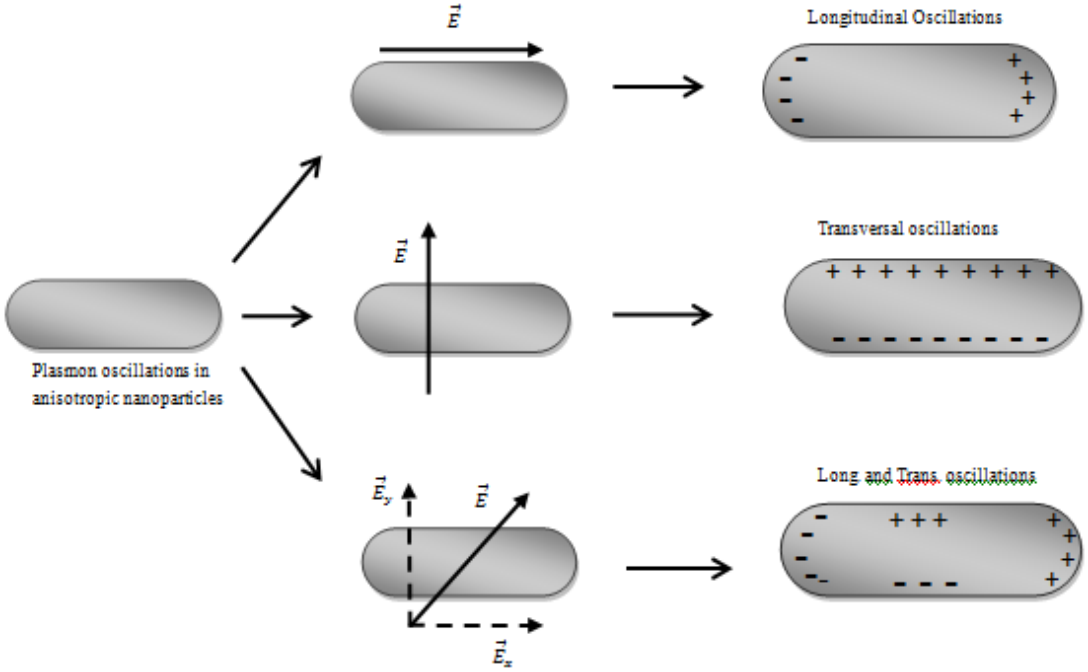

Fig.5. Schematic showing the transverse and longitudinal mode of oscillations of plasmons depending on the direction of electric vector of incident light

V. CONCLUDING REMARKS

We recall that the aim of this work was to study the optical and dielectric properties of single GNRs embedded in a dielectric medium, for this we have established a series of 3D-simulations using FEM to calculating the real and imaginary part of effective dielectric permittivity and the absorption cross-section.

First, we studied the effect of the major axis orientation of the GNR without shells relative to the direction of the external electric field, the results show that the properties of the SPR-peak and the complex dielectric permittivity depends on the polarization angle between the major axis of GNR and the external polarization direction. The real part of the dielectric permittivity takes the negatives values in a wavelengths range of the incident light, this range is broadest when the angle between the major axis of the GNR and the polarization direction is approaching to $\theta = 0°$ and vanished from a threshold value here $\theta \approx 62°$. The absorption spectra show that when the polarization angle is equal to $\theta = 0°$ only the longitudinal surface plasmons are excited and the SPR-peak position appeared towards the IR wavelengths, while when $\theta = \frac{\pi}{2}$ this is to say, the polarization field is perpendicular to the major axis of the GNR, in this case only the transverse plasmon is excited, and the resonance peak appeared toward the blue wavelengths. Between these two extremes cases, where the polarization direction is inclined relative to the major axis direction of the GNR, the two longitudinal and transverse modes are excited which leads to appearance of two resonance peaks. In this case, when the polarization angle increases the SPR-peak position of the longitudinal mode is red-shift and its amplitude decreases while the resonance peak of transverse mode does not change.

Finally, we emphasize that the numerical method developed in this work, for the investigation of the optical properties of the assembled coated GNPs, can be extended to other types of Gold nanoparticles, such as noble metallic nanoalloys of different shapes and morphology in order to improve the optical properties suitable for the biomedical applications.

REFERENCES

[1] U. Kreibig, M. Vollmer, *Optical Properties of Metal Clusters*, Springer-Verlag: Berlin, 1996.

[2] Y. Xia, N. Halas, "Shape-Controlled Synthesis and Suface Plasmonic Properties of Metallic Nanostructures," *Eds. MRS Bull*., vol. 30 (5) pp 338-344, 2005.

[3] L. M. Liz- Marzán, "Tailoring Surface Plasmons through the Morphology and Assembly of Metal Nanoparticles," *Langmuir*, vol. *22*(1), pp. 32–41, 2006.

[4] S. Link, and M. A. El-Sayed, "Shape and size dependence of radiative, non-radiative and photothermal properties of gold nanocrystals," *Int. Rev. Phys. Chem.*, Vol. 19, pp. 409–453, 2000.

[5] C.-H. Chou, C.-D. Chen and C. R. C. Wang, "Highly efficient, wavelength-tunable, gold nanoparticle based optothermal nanoconvertors," *J. Phys. Chem. B*, vol. 109, pp. 11135–11138, 2005.

[6] H. Petrova, J. P. Juste, I. Pastoriza-Santos, G. V. Hartland, L. M. Liz- Marzán and P. Mulvaney, "On the temperature stability of gold nanorods: Comparison between thermal and ultrafast laser-induced heating," *Phys. Chem.*, Vol. 8, pp. 814–821, 2006.

[7] L. R. Hirsch, R. J. Stafford, J. A. Bankson, S. R. Sershen, B. Rivera, R. E. Price, J. D. Hazle, N. J. Halas and J. L. West, "Nanoshell-mediated near-infrared thermal therapy of tumors under magnetic resonance guidance," *Proc. Natl Acad. Sci. USA*, vol. 100, pp. 13549–13554, 2003.

[8] C. M. Pitsillides, E. K. Joe, X. Wei, R. R. Anderson and C. P. Lin ,"Selective cell targeting with light-absorbing microparticles and nanoparticles," *Biophys. J.*, vol. 84, pp. 4023–4032, 2003.

[9] D. P. O'Neal, L. R. Hirsch, N. J. Halas, J. D. Payne and J. L. West, "Photo-thermal tumor ablation in mice using near infraredabsorbing nanoparticles," *Cancer Lett.*, Vol. 209, pp. 171–176, 2004.

[10] C. Loo, A. Lowery, J. West, N. Halas and R. Drezek, "Immunotargeted nanoshells for integrated cancer imaging and therapy," *Nano Lett.*, Vol. 5, pp. 709–711, 2005.

[11] H. El-Sayed, X. Huang and M. A. El-Sayed, "Selective laser photo-thermal therapy of epithelial carcinoma using anti-EGFR antibody conjugated gold nanoparticles," *Cancer Lett.*, Vol. 239, pp. 125–139, 2005.

[12] V. P. Zharov, R. R. Letfullin and E. N. Galitovskaya, "Microbubbles-overlapping mode for laser killing of cancer cells with absorbing nanoparticle clusters," *J. Phys. D*, vol. 38, pp. 2571–2581, 2005.

[13] X. Huang, I. H. El-Sayed, W. Qian and M. A. El-Sayed, "Cancer cell imaging and photothermal therapy in the nearinfrared region by using gold nanorods," *J. Am. Chem. Soc.*, Vol. 128, pp. 2115–2120, 2006.

[14] H. El-Sayed, X. Huang and M. A. El-Sayed, "Selective laser photo-thermal therapy of epithelial carcinoma using anti-EGFR antibody conjugated gold nanoparticles," *Cancer Lett.*, Vol. 239, pp. 129–135, 2006.

[15] T. B. Huff, L. Tong, Y. Zhao, M. N. Hansen, J.-X. Cheng and A. Wei, "Hyperthermic effects of gold nanorods on tumor cells," *Nanomedicine*, vol. 2, pp. 125–132, 2007.

[16] L. Tong, Y. Zhao, T. B. Huff, M. N. Hansen, A. Wei and J.-X. Cheng, "Gold nanorods medicate tumor cell death by compromising membrane integrity," *Adv. Mater*, vol. 19, pp. 3136–3141, 2007.

[17] J. Chen, D. Wang, J. Xi, L. Au, A. Siekkinen, A. Warsen, Z. Y. Li, H. Zhang, Y. Xia and X. Li, "Immuno gold nanocages with tailored optical properties for targeted photothermal destruction of cancer cells," *Nano Lett.*, Vol. 7, pp. 1318–1322, 2007.

[18] P. Wust, B. Hildebrandt, G. Sreenivasa, B. Rau, J. Gellerman, H. Riess, R. Felix and P. M. Schlag, "Hyperthermia in combined treatment of cancer," *Lancet Oncol*, vol. 3, pp. 487–497, 2002.

[19] I. Sherman, and M. Ter-Pogossian, "Lymph-node concentration of radioactive colloidal gold following interstitial Injection," *Cancer*, vol. 6, pp. 1238–1240, 1953.

[20] B. Nikoobakht, and M. A. El-Sayed, "Preparation and growth mechanism of gold nanorods (NRs) using seed-mediated growth method," *Chem. Mater*, vol. 15, pp. 1957–1962, 2003.

[21] T. K Sau. and C. J. Murphy, "Seeded high yield synthesis of short Au nanorods in aqueous solution," *Langmuir*, vol. 20, pp. 6414–6420, 2004.

[22] K. Imura, T. Nagahara and H. Okamoto, "Near-field twophoton-induced photoluminescence from single gold nanorods and imaging of plasmon modes," *J. Phys. Chem. B*, vol. 109, pp. 13214–13220, 2005.

[23] M. Pelton, M. Liu, H. Y. Kim, G. Smith, P. Guyot-Sionnest and N. F. Scherer, "Optical trapping and alignment of single gold nanorods by using plasmon resonances," *Opt. Lett.*, Vol. 31, pp. 2075–2077, 2006.

[24] G. Mie, "Beitrage zur Optik truber Medien, speziell kolloidaler Metallosungen," *Ann. Phys.*, vol. 25, pp. 377-445, 1908.

[25] U. Kreibig, U. Genzel, "Optical absorptionof small metallic particles," Surf. Sci., 156, pp. 678-700, 1985.

[26] M. Cini, "Classical and quantum aspects of size effects," *J. Opt. Soc. Am.*, vol. 71, pp. 386-392, 1981.

[27] R. Gans, "Form of ultramicroscopic particles of silver," *Ann. Phys.*, vol. 47, pp. 270–284, 1915.

[28] C.F. Bohren and D.R. Huffman, *Absorption and Scattering of Light by Small Particles*, John Wiley, New York, 1983.

[29] J. C. Maxwell Garnett, "Colours in metal glasses and in metallic films," *Phil. Trans. R. Soc. London A*, vol. 203, pp. 385-420, 1904.

[30] C.A. Foss, G.L. Hornyak, M.J. Tierney and C.R. Martin, "Template synthesis of infrared-transparent metal microcylinders: comparison of optical properties with the predictions of effective medium theory," *J. Phys. Chem.*, vol. 96, pp 9001–9007, 1992.

[31] C.A. Foss, G.L. Hornyak, J.A. Stockert and C.R. Martin, "Template-Synthesized Nanoscopic Gold Particles: Optical-Spectra and the Effects of Particle-Size and Shape," *J. Phys. Chem.*, vol. 98, pp.2963-2971, 1994.

[32] G. L. Hornyak, C. J.Patrissi and C. R.Martin, "Fabrication, Characterization and Optical Properties of Gold-Nanoparticle/Porous-Alumina Composites: The Non-Scattering Maxwell-Garnett Limit," *J. Phys. Chem B.*, vol. 101, pp. 1548-1555, 1697.

[33] G. L. Hornyak, C. R.Martin, "Optical Properties of a Family of Au-Nanoparticle-Containing Alumina Membranes in which the Nanoparticle Shape Is Varied from Needle-Like (Prolate) to Spheroid, to Pancake-Like (Oblate)," *Thin Solid Films*, vol. 300, pp. 84-88, 1997.

[34] J.N. Reddy, *An Introduction to Finite Element Method*, 2nd., Mc Graw Hill, New York, 1993; See also O.C. Zienkiewicz and R.L. Taylor, *The Finite Element Method*, Vol. 1, McGraw-Hill, London, 1989.

[35] M. Benhamou, A.R. Senoudi, F. Lallam, A. Boussaid and A. Bensafi, "Optical Properties Of Anisotropic Nanogolds From Finite Element Method," *Science & Nano Technology: An Indian Journa*l, vol. 4, 2010.

[36] A.Akouibaa, M. Benhamou, A. Derouiche, "Simulation of the Optical Properties of Gold Nanorods: Comparison to Experiment", *IJARCSSE*., vol. 3(9), pp. 657-671, 2013.

[37] A.Akouibaa, A. Derouiche, H. Ridouane, A. Bettachy, F. Benzouine, "Numerical Study of Optical Properties of Tow Assembled Gold Core/Polymer-Shell Nanoparticles in Dielectric Medium," *IJARCSSE Journal*, accepted (Paper ID: V4I3-0160), 2013.

[38] N.K. Grady, N.J. Halas, P. Nordlander, "Influence of dielectric function properties on the optical response of plasmon resonant metallic nanoparticles," *Chemical Physics Letters*, vol. 399, pp. 167-171, 2004.

[39] E. Neeves and M.N.Birnboim, "Composite Structure for the enhancement of nonlinear-optical susceptibility," *J.Opt Soc. Am. B*, Vol. 6, N. 4, April 1989.

[40] B. Lucia Scaffardi and J. O. Tocho, "Size dependence of refractive index of gold nanoparticles," *Institute Of Physics Publishing, Nanotechnology*, vol. 17, pp. 1309–1315, 2006.

[41] R. D. Averitt, D. Sarkar, and N. J. Halas, "Plasmon Resonance Shifts of Au-Coated Au2S Nanoshells: Insight into Multicomponent Nanoparticle Growth," *Phys Rev Lett*., Vol. 78, N. 22, June 1997.

[42] P.G. Etchegoin, E.C.L. Ru and M.Meyer, "An analytic model for the optical properties of gold," *J. Chem. Phys.*, vol. 125, pp. 164705-164708, 2006.

[43] F.Hao and P.Nordlander, "Efficient dielectric function for FDTD simulation of the optical properties of silver and gold nanoparticles," *Chem.Phys. Lett*., vol. 446, pp. 115-118, 2007.

[44] Vial and T. Laroche, "Comparison of gold and silver dispersion laws suitable for FDTD Simulations," *Appl.Phys.B: Laser Opt*., vol. 93, pp. 139-143, 2008.

[45] V. Myroshnychenko and C. Brosseau, "Finite-element method for calculation of the effective permittivity of random inhomogeneous media," *Phys. Rev. E*., vol. 7, pp. 016701-016716, 2005.

[46] N. Jebbor and S. Bri, "Effective permittivity of periodic materials: Numerical modeling by the finite element method," *J. of Electrostatics*, vol. 70, pp. 393-399, 2012.

[47] B. Sareni, L Krähenbühl, A. Beroual, and C. Brosseau, "Effective dielectric constant of periodic composite materials," *J. Appl. Phys*., vol. 80(3), pp. 1688-1696, 1996.

[48] K. Ghosh and M. E. Azimi, "Numerical calculation of effective permittivity of lossless dielectric mixture using Boundary Integral Method," *IEEE Trans. on Diel. and Elect. Insul*., vol. 1, pp. 975- 981, 1994.

[49] G. Weick, R.A. Molina, D. Weinmann and R.A. Jalabert, "Life time of the first and second collective excitations in metallic nanoparticles," *Phys. Rev. B*, vol. 72, pp. 115410-1-17, 2005.

[50] E.D. Palik, *Handbook of Optical Constants of Solids III*, Academic Press, New York, 1991.

[51] V. G. Veselago, "Electrodynamics of substances with simultaneously negative electrical and magnetic permeabilities," *Sov. Phys. Usp*., vol. 10, pp. 509-514. 1968.

[52] R. A. Shelby, D. R. Smith and S. Schultz, "Experimental Verification of a Negative Index of Refraction," *Science*, vol. 292, pp. 77-79, 2001.

[53] Q. Liu, Y. Cui, D. Gardner, X. Li, S. He, and I. I. Smalyukh, "Self-Alignment of Plasmonic Gold Nanorods in Reconfigurable Anisotropic Fluids for Tunable Bulk Metamaterial Applications," *Nano Lett*., vol. 10, pp. 1347–1353, 2010.

[54] C. Khoo, D. H. Werner, X. Liang, A. Diaz, and B. Weiner, "Nanosphere dispersed liquid crystals for tunable negative–zero–positive index of refraction in the optical and terahertz regimes," *Optics Letters*, Vol. 31, Issue 17, pp. 2592-2594, 2006.

